

Assessment of Antiangiogenic Effect Using ^{99m}Tc -EC-Endostatin

David J. Yang,^{1,2} Kil-Dong Kim,³ Naomi R. Schechter,⁴ Dong-Fang Yu,² Peng Wu,²

Ali Azhdarinia,² Jennifer S. Roach,³ Saady K. Kalimi,² Kaoru Ozaki,² William E. Fogler,⁵

Jerry L. Bryant,² Roy Herbst,³ James Abbruzzes,³ E. Edmund Kim,² Donald A. Podoloff²

Departments of Nuclear Medicine² and Thoracic/Head & Neck Medical Oncology³ and Radiation Oncology,⁴ The University of Texas M. D. Anderson Cancer Center,¹⁻⁴ Houston, Texas and EntreMed, Inc.,⁵ Rockville, Maryland

Purpose. Tumor vascular density may provide a prognostic indicator of metastatic potential or survival. The purpose of this study was to develop ^{99m}Tc -ethylenedicysteine-endostatin (^{99m}Tc -EC-endostatin) for the evaluation of anti-angiogenesis therapy. **Method.** ^{99m}Tc -EC-endostatin was prepared by conjugating ethylenedicysteine (EC) to endostatin, followed by adding pertechnetate and tin chloride. Radiochemical purity was >95%. In vitro cell viability, affinity and TUNEL assays were performed. Tissue distribution and planar imaging of radiolabeled endostatin were determined in tumor-bearing rats. To assess anti-angiogenic treatment response, rats were treated with endostatin, paclitaxel and saline, followed by imaging with ^{99m}Tc -EC-endostatin. Tumor response to endostatin therapy in tumor-bearing animal models was assessed by correlating tumor uptake dose with microvessel density, VEGF, bFGF and IL-8 expression during endostatin therapy. **Results.** In vitro cell viability and TUNEL assays indicated no marked difference between EC-endostatin and endostatin. Cellular uptake assay suggests that endostatin binds to endostatin receptor. Biodistribution of ^{99m}Tc -EC-endostatin in tumor-bearing rats showed increased tumor-to-tissue count density ratios as a function of time. Tumor uptake (%ID/g) of ^{99m}Tc -EC-endostatin was 0.2–0.5. Planar images confirmed that the tumors could be visualized clearly with ^{99m}Tc -EC-endostatin. The optimal time for imaging using radiolabeled endostatin was 2 hrs. ^{99m}Tc -EC-endostatin could assess treatment response. There was a correlation between tumor uptake and cellular targets expression. **Conclusion.** The results indicate that it is feasible to use ^{99m}Tc -EC-endostatin to assess efficiency of anti-angiogenesis therapy.

Key Words: ^{99m}Tc -EC-endostatin, antiangiogenesis, biodistribution, imaging

INTRODUCTION

Angiogenesis, the proliferation of endothelial and smooth muscle cells to form new blood vessels, is an essential component of the metastatic pathway. These vessels provide the principal route by

which tumor cells exit the primary tumor site and enter the circulation. For many tumors, the vascular density can provide a prognostic indicator of metastatic potential or survival, with highly vascularized tumors having a higher incidence of metastasis than poorly vascularized tumors.¹⁻³

It may be feasible to block angiogenesis and tumor progression by using anti-angiogenic agents. At present, antiangiogenic agents under clinical testing include: naturally occurring inhibitors of angiogenesis (e.g., angiostatin, endostatin, platelet factor-4),⁴⁻⁷ specific inhibitors of

Address reprint requests to Dr. David J. Yang, University of Texas M. D. Anderson Cancer Center, Department of Nuclear Medicine, Box 59, 1515 Holcombe Boulevard, Houston, Texas 77030 Tel: (713) 794-1053 Fax: (713) 794-5456 E-mail: dyang@di.mdacc.tmc.edu

endothelial cell growth (e.g., TNP-470, thalidomide, interleukin-12),⁸⁻¹⁰ agents neutralizing angiogenic peptides (e.g., antibodies to fibroblast growth factor or vascular endothelial growth factor, suramin and analogues, tecogalan)¹¹⁻¹² or their receptors,¹³ agents that interfere with vascular basement membrane and extracellular matrix (e.g., metalloprotease inhibitors, angiostatic steroids),¹⁴⁻¹⁶ anti-adhesion molecules,¹⁷ antibodies such as anti-integrin $\alpha_v\beta_3$,¹⁸ and miscellaneous drugs that modulate angiogenesis by diverse mechanisms of action.¹⁹

Malignant tumors are angiogenesis-dependent. Several experimental studies suggest that primary tumor growth, invasiveness and metastasis require neovascularization.²⁰⁻²² Tumor-associated angiogenesis is a complex, multistep process under the control of positive and negative soluble factors. Acquisition of the angiogenic phenotype is a common pathway for tumor progression, and active angiogenesis is associated with molecular mechanisms leading to tumor progression.²³ For instance, vascular endothelial growth factor (VEGF) is a mitogen, morphogen and chemoattractant for endothelial cells and, *in vivo*, is a powerful mediator of vessel permeability.²⁴ Interleukin-8 (IL-8) is a chemo-attractant for neutrophils and is a potent angiogenic factor.²⁵ Basic fibroblast growth factor (bFGF) has been associated with tumorigenesis and metastasis in several human cancers.²⁶ The prognostic value of angiogenesis factor expression (e.g., VEGF, bFGF, microvessel density, IL-8, MMP-2 and MMP-9) has been determined for cancer patients treated with chemotherapy.^{27,28} These factors regulate metastasis and angiogenesis and may predict the metastatic potential in individual cancer patients.²⁹

The use of anti-angiogenic therapy agents, such as endostatin, represents one of the more promising new approaches to anti-cancer therapy. Endostatin, a fragment of the COOH-terminal domain of mouse collagen XVIII, is an endogenous inhibitor of tumor angiogenesis and endothelial cell growth. Treatment of cow pulmonary artery endothelial cells with endostatin has been shown to cause apoptosis. Furthermore, addition of endostatin led to a marked reduction of the Bcl-2 and Bcl-XL anti-apoptotic proteins, whereas Bax (pro-apoptotic) protein levels were unaffected.⁵ These effects were not seen in several non-endothelial cells.³⁰⁻³⁴ Though angiogenic factors reflect angiogenesis status, these agents may not adequately reflect the therapeutic response of tu-

mors. Currently, methods of assessing angiogenesis in tumors rely on counting microvessel density in the areas of neovascularization. After tissue biopsy, immunohistochemistry of tissue specimen is performed. The technique is invasive and can not be repeatedly performed. Thus, the development of noninvasive imaging techniques to measure anti-angiogenic effects would be a welcome contribution to the clinical arsenal.

Radionuclide imaging modalities (positron emission tomography, PET; single photon emission computed tomography, SPECT) are diagnostic cross-sectional imaging techniques that map the location and concentration of radionuclide-labeled radiotracers. Although computed tomography (CT) and magnetic resonance imaging (MRI) provide considerable anatomic information about the location and the extent of tumors, these imaging modalities cannot adequately differentiate invasive lesions from edema, radiation necrosis, grading, or gliosis. PET and SPECT have been used to localize and characterize tumors by measuring functional and metabolic activities. They have been also utilized in differentiating malignant and benign lesions, evaluating and predicting therapeutic responses.³⁵⁻³⁸

Due to favorable physical characteristics, easy availability, and low price (\$0.21/mCi vs. \$50/mCi of ¹⁸F), ^{99m}Tc is an agent of choice for labeling radiopharmaceuticals. ^{99m}Tc-ethylenedicycysteine (^{99m}Tc-EC) is a successful example of a stable N₂S₂ chelate.³⁹ Using a standard coupling technique, ^{99m}Tc-EC-drug conjugates have been developed to characterize tumors.³⁹⁻⁴² This method may become a universal technique to evaluate various molecular targets for cancer diagnosis.

Although endostatin causes endothelial apoptosis,⁵ the exact mechanism of endostatin binding has not been elucidated. Our hypothesis states that endostatin may bind to endostatin receptors and that this binding reflects therapeutic response. If the uptake of tumor endothelial cells can be assessed by ^{99m}Tc-EC-endostatin using planar scintigraphy, this agent could be used to evaluate the efficiency of endostatin therapy for cancer. Assessing angiogenesis in tumors with ^{99m}Tc-EC-endostatin may prove to be a rational means of selecting patients for treatment with anti-angiogenic agents. In this report, *in vitro* cellular uptake assay, biodistribution, imaging studies, and anti-angiogenic therapy studies using ^{99m}Tc-EC-endostatin in mammary tumor-bearing

rats were evaluated. Further, tumor uptake and expression of various angiogenic factors (tumoral VEGF, bFGF, IL-8, and microvessel density) were correlated.

MATERIALS AND METHODS

Synthesis of L,L-Ethylenedicysteine (EC)

EC was prepared in a two-step synthesis according to previously described methods.²⁵ Briefly, the precursor, L-thiazolidine-4-carboxylic acid (m.p. 195°, reported 196–197°), was synthesized by reacting cysteine with formaldehyde. EC (m.p. 243°C, reported 251°C) was then prepared via reduction of L-thiazolidine-4-carboxylic acid in liquid ammonia and sodium.

Synthesis of ^{99m}Tc-EC-endostatin

Sodium bicarbonate (1N, 1 mL) was added to a stirred solution of EC (391 mg, 1.46 mmol). To this colorless solution, sulfo-N-hydroxysulfosuccinimide (Pierce Chemical Co., Radford, IL) (313 mg, 1.46 mmol) and 1-ethyl-3-(3-dimethylaminopropyl) carbodiimide (EDC, 313 mg, 1.9 μmol) (Aldrich Chemical Co., Milwaukee, WI) were added. Endostatin (Entremed, Inc., Rockville, MD) (15 mg, 0.75 μmol) was then added. The mixture was stirred at room temperature for 24 hrs. The mixture was dialyzed for 48 hrs (M.W. cut-off of 10,000). EC-endostatin weighed 17 mg (yield: 100%) after freeze drying. ^{99m}Tc-pertechnetate (5.5 mCi) (Syncor Pharmaceutical Inc., Houston, TX) was added to a vial containing the lyophilized residue of EC-endostatin (10 μg, 0.5 nmol) and tin chloride (II) (SnCl₂, 100 μg, 0.53 μmol) in 0.2 mL water. The product was purified by using a sephadex G-25 column (bedvolume 10 mL) (Sigma Chemical Company, St. Louis, MO) and eluted with PBS (5 mL). One mL of eluent was collected in each test tube. The product was isolated in Tubes 3 and 4, yielded 3.9 mCi (70%). Radiochemical purity was assessed by Radio-TLC scanner (Bioscan, Washington, DC) using 1M ammonium acetate : methanol (4:1) as an eluant. High performance liquid chromatograph (HPLC), equipped with a GPC column (Biosep SEC-S3000, 7.8 × 300 mm, Phenomenex, Torrance, CA) and two detectors (NaI and UV), was used to analyze the purity of the product. The eluant was 0.1% LiBr in PBS (10 mM) and the flow rate was 1.0 mL/min.

The stability of labeled endostatin was tested in serum samples. Briefly, labeled endostatin (100 μCi) was incubated in dog serum (200 μL) at 37°C at 0.5–24 hrs. The serum samples were diluted with 50% methanol in water and radio-TLC was used to analyze the product.

In Vitro Cell Viability Studies

To determine whether EC-endostatin acts like endostatin, *in vitro* potency was evaluated in RBA CRL-1747 rat breast cancer cell line (American Type Culture Collection, Rockville, MD). This cell line was derived from a tumor induced in a Fischer-344 rat by giving an oral dose of 7,12-dimethyl-benz[a]anthracene. This cell line is known to respond to endostatin treatment.⁴³ Cells (5,000/well, 96-well plate) were treated with various doses (0.1–100 μM) of EC-endostatin and endostatin. The cells were incubated for 3 days at 37°C. Cell viability was determined by an MTT assay.⁴²

Immunofluorescence double staining deoxynucleotidyl transferase-mediated 2'-deoxyuridine 5'-triphosphate-biotin nick end labeling (TUNEL) cell assay was used to evaluate EC-endostatin induced apoptosis. Briefly, sparse cultures of human dermal microvascular endothelial cells-HD-MEC-nd (Cascade Biologics, Portland, OR) were plated in 2-well chamber slides and allowed to attach for 24 hrs. They were incubated over 18 hrs at 37°C with 2 mg/mL endostatin, EC-endostatin or EC alone. TUNEL was performed using a commercially available apoptosis detection kit (Promega Corporation, Madison WI). A mounting medium-containing propidium iodide (Vector Laboratories, Burlingame, CA) was used to coverslip the samples. Immunofluorescence microscopy was performed using a 20×-objective (Zeiss Plan-Neoplur) on an epifluorescence microscope equipped with narrow bandpass excitation filters mounted in a filter wheel (Ludl Electronic Products, Hawthorne, NY) to individually select for green and red fluorescence. Images were captured using a cooled CCD camera (Photometrics, Tucson, AZ) and SmartCapture software (Digital Scientific, Cambridge, England) on a Macintosh computer. Images were subsequently processed using Adobe Photoshop software (Adobe Systems, Mountain View, CA). Endothelial cells were identified by red fluorescence and DNA fragmentation was detected by localized yellow and green fluorescence within the nucleus of apoptotic endothelial cells. Quantifica-

tion of apoptotic endothelial cells was expressed as an average of apoptotic cells to the total number of endothelial cells in 10 random 0.24 mm² fields at 200× magnification. Triplicate assays were performed and total TUNEL expression was given as the average.

***In Vitro* Cell Affinity Studies**

Cellular binding was evaluated in the RBA CRL-1747 rat breast cancer cell line to determine whether ^{99m}Tc-EC-endostatin binds to endostatin receptors. Cells (33,000/well) were treated with various doses (0–16 μM/well) of endostatin and ^{99m}Tc-EC-endostatin (0.31 μM/well, 0.1 μCi/well). After 2 hrs incubation, the cells were washed twice with ice cold PBS (1 mL), and trypsin EDTA (0.1 mL) was added. After 2 min, PBS (0.4 mL) was added and the total volume containing cells was transferred to a test tube to count the activity. Cell viability was determined by an MTT assay as described previously. Each data represents an average of three measurements and that were calculated as percentage of uptake per number of viable cells.

Tissue Distribution Studies

Eighteen female Fischer 344 rats (150 ± 25 g) (Harlan Sprague-Dawley, Indianapolis, IN) (n = 3 rats/time point) were inoculated (i.m.) with mammary tumor cells derived from the RBA CRL-1747 cell line. The cells were cultured in Eagle's MEM with Earle's BSS (90%) and fetal bovine serum (10%). Tumor cells (10⁶ cells/rat) were injected (i.m.) into the hind legs. Studies were performed 14 to 17 days after implantation when tumors were approximately 1 cm in diameter.

In tissue distribution studies, each animal was injected (i.v., 10 μCi/rat, 10 μg/rat) with ^{99m}Tc-EC-endostatin or ^{99m}Tc-EC. Rats were sacrificed at 0.5–4 hrs. The selected tissues were excised, weighed and counted for radioactivity by using a gamma counter (Packard Instruments, Downers Grove, IL). The biodistribution of tracer in each sample was calculated as percentage of the injected dose per gram of tissue wet weight (%ID/g).

Scintigraphic Imaging Studies

Scintigraphic images, using a gamma camera (Siemens Medical Systems, Inc., Hoffman Estates, IL) equipped with low-energy, parallel-hole

collimator, were obtained at 0.5–4.0 hrs after i.v. injection of each radiotracer, respectively. To ascertain whether the tumor uptake by with ^{99m}Tc-EC-endostatin was related to endostatin receptor, we performed a blocking study. Each rat was pretreated with endostatin (n = 3, 50 mg/kg, iv) 1 hr prior to receiving ^{99m}Tc-EC-endostatin (300 μCi/rat, iv) and imaged at 0.5–4.0 hrs. In a separate study, rats (n = 3) received ^{99m}Tc-EC-K1XaK2tPA (Entremed, Rockville, MD). K1XaK2tPA is a human plasminogen peptide with molecular size of 20 kDa which is similar to endostatin.⁴⁴ This peptide was used as a non-specific control. Computer outlined regions of interest (ROI) (counts per pixel) were used to determine tumor-to-background count density ratios.

Therapeutic Response Assessment

Mammary tumor-bearing rats (n = 5 rats/agent) received (i.v.) endostatin (50 mg/kg), paclitaxel (20 mg/kg), or saline. After one week, tumor-bearing rats were imaged with ^{99m}Tc-EC-endostatin at 0.5–4.0 hrs. Computer outlined regions of interest (ROI) (counts per pixel) of tumor lesion site and symmetric normal muscle site was used to determine tumor-to-background count density ratios. The ratios were used to compare dynamic tumor uptake pre- and post-treatment. ROI changes have been used as a standard to correspond to anatomically relevant features.^{45,46}

In-Situ Hybridization (ISH) Assays

To determine whether tumor uptake of ^{99m}Tc-EC-endostatin correlates with mRNA expression in the tumor specimen of rats, ISH was performed.^{47–50} ISH was carried out using the Microprobe manual staining system (Fisher Scientific, Pittsburgh, PA), which detects hybridization of a biotinylated DNA probe with mRNA. Tissue sections (4 μm) of formalin-fixed, paraffin-embedded specimens were mounted on silane-coated slides. The slides were placed in the Microprobe slide holder, dewaxed, and dehydrated with alcohol followed by enzymatic digestion with pepsin.⁵¹ Hybridization of the biotinylated DNA probe was carried out for 60 min at 45°C. The samples were incubated for 30 min in alkaline phosphatase-labeled avidin at 45°C, briefly rinsed in 50 mM Tris buffer (pH 7.6), rinsed for 1 min with alkaline phosphatase enhancer (Biomedica Corp., Foster City, CA), and incubated for 30 min with the chromogen substrate FastRed at 45°C. A positive reaction in this as-

say stained red. Control for endogenous alkaline phosphatase included treatment of the samples in the absence of the biotinylated probe and use of chromogen in the absence of any oligonucleotide probes. To check the specificity of the hybridization signal, the following controls were used: (1) Rnase pretreatment of tissue sections, (2) a biotin-labeled sense probe, and (3) a competition assay with unlabeled antisense probe.

To assess microvessel density changes,⁵² anti-CD-31 immunohistochemical analysis was performed. Briefly, fresh frozen tumor specimens were prepared and stained with anti-CD-31 antibodies. The vessels were imaged with a fluorescence microscope. Vessel density was analyzed by quantifying PE-positive pixels per recorded field. Histopathology of VEGF, microvessel density, IL-8 and bFGF from tumor specimen obtained on days 1, 2, 4 and 7 post-treatment of endostatin were performed.

RESULTS

Chemistry

EC, a dicarboxylic acid chelator, may be conjugated to amino or lysine residues of endostatin. From the reaction yield (70–75%), ten EC residues was estimated to conjugate to endostatin (M.W. 20 kDa). ^{99m}Tc-EC-endostatin was found to be radiochemically pure (>97%) (Figure 1). The retention time of ^{99m}Tc-EC-endostatin was 10.7 min. The amount of ^{99m}Tc-EC-endostatin injected to HPLC was 1 μ Ci per 22.5 ng. The specific activity was calculated to be 1 Ci/ μ mol. Under the same condition, the retention time of ^{99m}Tc-EC and endostatin was 2 min and 10.3 min. Using radio-TLC analysis of ^{99m}Tc-EC-endostatin, there was no difference in retardation factor ($R_f = 0.4$) at various incubation times, suggesting its *in vivo* stability (results not shown). Together, these results suggest that this

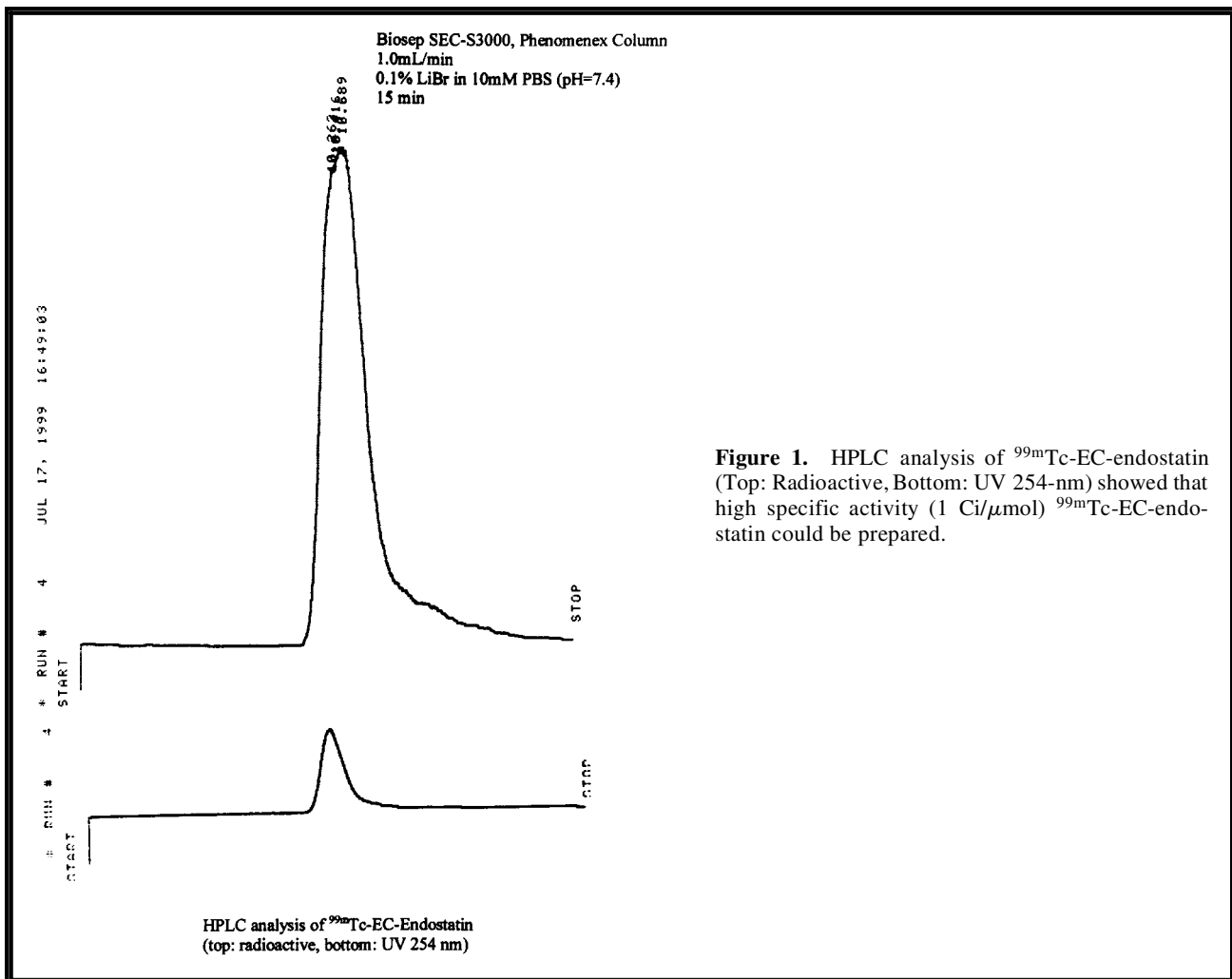


Figure 1. HPLC analysis of ^{99m}Tc-EC-endostatin (Top: Radioactive, Bottom: UV 254-nm) showed that high specific activity (1 Ci/ μ mol) ^{99m}Tc-EC-endostatin could be prepared.

methodology results in a simple and efficient synthesis of ^{99m}Tc -EC-endostatin.

In Vitro Cell Viability and Cell Affinity Studies

Cell viability assays showed no marked difference between EC-endostatin and endostatin (Figure 2). At higher dose ($>100\ \mu\text{M}$), significant cell death was observed in both groups. There was an unexpected drop in % inhibition curve, which might be due to experimental error. TUNEL assays showed that EC-endostatin and endostatin caused $19.87 \pm 0.36\%$ and $19.43 \pm 0.67\%$ cell apoptosis, respectively. There was no marked difference between EC-endostatin and endostatin groups (Figure 3).

In *in vitro* cell affinity assays, there was a markedly decreased uptake (20–50%) of ^{99m}Tc -EC-endostatin after adding excess unlabeled endostatin (Table 1). We hypothesize that this decreased uptake might be due to the specific binding of endostatin to endostatin receptors.

In Vivo Biodistribution Studies

Tumor-to-tissue uptake ratios for ^{99m}Tc -EC-endostatin groups increased as a function of time when compared to ^{99m}Tc -EC (Tables 2 and 3). The time for the optimal uptake of endostatin in tumors was 2–4 hrs postinjection of ^{99m}Tc -EC-endostatin. Tumor uptake (%ID/G) in ^{99m}Tc -EC-endostatin groups was higher than ^{99m}Tc -EC (Table 3). Liver uptake in ^{99m}Tc -EC-endostatin groups was higher than ^{99m}Tc -EC groups. The difference in liver uptake may be due to different molecular weight (M.W. 20 kDa of endostatin vs. M.W. 268 of EC). High kidney uptake was observed for both ^{99m}Tc -EC and ^{99m}Tc -EC-endostatin groups (9.2 ± 0.05 and $25.7 \pm 0.83\% \text{ID/g}$ at 2 hrs, respectively), presumably because these agents are excreted through the kidney.

Scintigraphic Imaging Studies

Scintigraphic images of rats given ^{99m}Tc -EC-endostatin demonstrated that tumors could be well

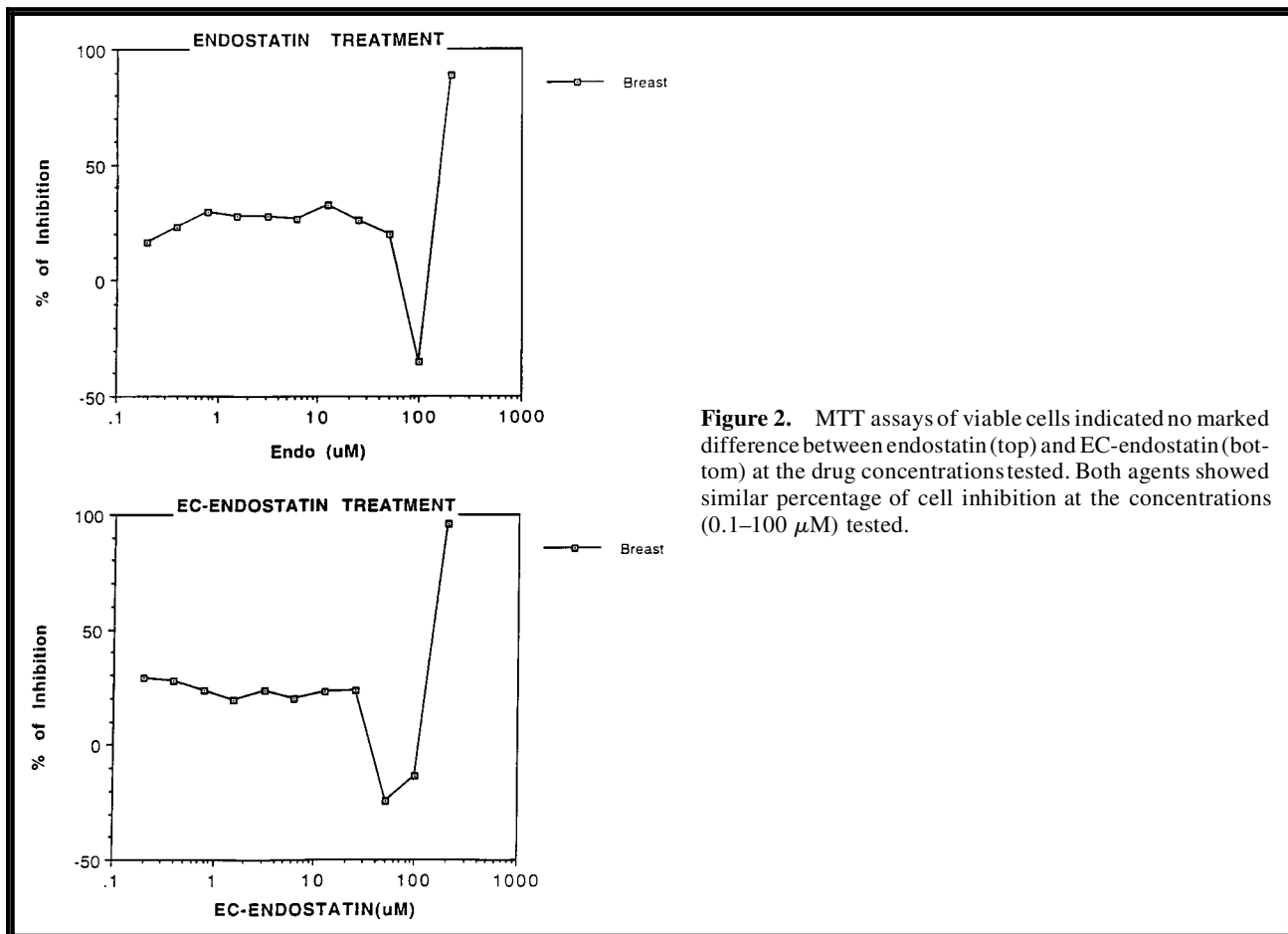
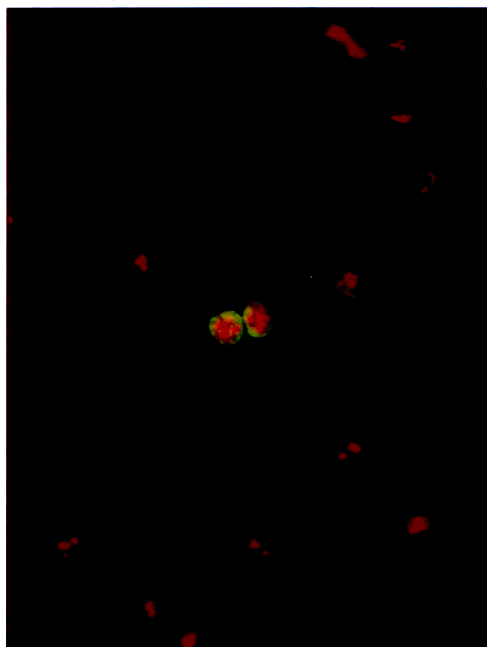


Figure 2. MTT assays of viable cells indicated no marked difference between endostatin (top) and EC-endostatin (bottom) at the drug concentrations tested. Both agents showed similar percentage of cell inhibition at the concentrations (0.1–100 μM) tested.

100 μ M EC-Endostatin



100 μ M Endostatin

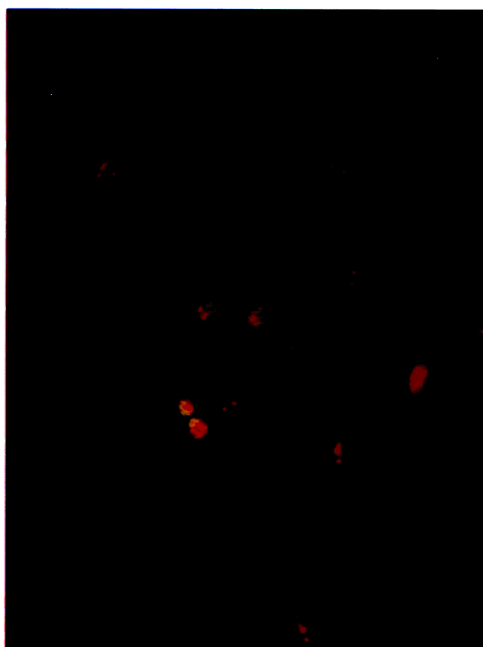


Figure 3. Immunofluorescence double staining of apoptotic human dermal microvascular endothelial cells (TUNEL assay) indicated no marked difference between EC-endostatin and endostatin at the drug concentration (2 mg/mL) tested. EC-endostatin and endostatin induced apoptosis in $19.9 \pm 0.36\%$ and $19.4 \pm 0.67\%$ of the cells, respectively.

visualized at 0.5–4.0 hrs 14 days after inoculation of tumor cells (Figure 4). *In vivo* blocking studies showed that there was 30–40% decreased uptake after pretreatment with unlabeled endostatin in molar excess (data not shown). Also, tumor had poor uptake (2–4 hrs) of ^{99m}Tc -EC-K1XaK2tPA, a non-specific peptide (Figure 5). The findings suggest that tumor uptake of ^{99m}Tc -

EC-endostatin may be via an endostatin receptor-mediated process.

Therapeutic Response Assessment

A curve showing anti-rat mammary tumor growth activity caused by paclitaxel and endostatin is presented in Figure 6. Scintigraphic images of

TABLE 1. Effect of Endostatin on Uptake of ^{99m}Tc -EC-Endostatin in Breast Tumor Cells¹

Endostatin Dose (μM)	% Uptake / Viable Cells* 10^6
Control	6.669 \pm 0.404
10	5.411 \pm 0.249 ²
12	3.076 \pm 0.036 ²
13	3.198 \pm 0.070 ²
16	3.539 \pm 0.206 ²

¹Cellular uptake was determined at 2 hr post-incubation. Each data represents an average of three measurements. Each data was calculated as %uptake/viable cells* 10^6 . The amount of ^{99m}Tc -EC-endostatin used was 0.31 μM /well, 0.1 μCi /well.

² $p < 0.05$ (compared to control group), student t-test

TABLE 2. Biodistribution of ^{99m}Tc-EC-Endostatin in Breast Tumor-Bearing Rats

	% of injected ^{99m} Tc-EC-Endostatin dose per gram of tissue weight ¹		
	30 min	2 h	4 h
Blood	1.042±0.027	0.420±0.039	0.254±0.006
Lung	0.615±0.015	0.298±0.017	0.208±0.008
Liver	2.415±0.103	1.506±0.183	1.387±0.038
Spleen	2.248±0.217	1.316±0.114	0.968±0.077
Kidney	22.993±0.672	25.733±0.832	25.426±0.298
Thyroid	0.892±0.061	0.375±0.006	0.359±0.018
Muscle	0.129±0.009	0.051±0.003	0.037±0.002
Intestine	0.320±0.008	0.173±0.010	0.142±0.011
Tumor	0.499±0.016	0.282±0.015	0.226±0.006
Brain	0.040±0.004	0.024±0.005	0.018±0.003
Urine	13.172±2.841	23.952±6.052	N/A ²
Tumor/Blood	0.480±0.017	0.676±0.034	0.891±0.006
Tumor/Muscle	3.901±0.346	5.509±0.071	6.062±0.186
Tumor/Lung	0.812±0.015	0.947±0.032	1.091±0.029

1. Each rat was given 10 µg of ^{99m}Tc-EC-Endostatin. Values shown represent the mean±standard deviation of data from 3 animals.

2. N/A: not available to collect.

^{99m}Tc-EC-endostatin demonstrated that the tumor could be well visualized on day 7 post-treatment with endostatin and paclitaxel. A selected image at 1 hour post-^{99m}Tc-EC-endostatin is shown in Figure 6. Tumor appeared to have higher uptake of ^{99m}Tc-EC-endostatin in the control (saline) group than in either of the groups treated with endostatin or paclitaxel. Using computer outlined ROI of the tumor lesion site and symmetric non-tumor muscle site, tumor to non-

tumor count density ratios for endostatin, paclitaxel and saline on day 7 post-treatment were calculated to be 2.40 ± 0.03 , 2.38 ± 0.03 , and 3.77 ± 0.04 , respectively. The weights of tumors at sacrifice were 5.5 ± 0.33 g, 3.1 ± 0.11 g, and 7.9 ± 0.42 g, respectively. There was 36% less uptake of ^{99m}Tc-EC-endostatin by tumor in the endostatin-treated group vs. the saline group (Figure 7). There was a correlation between this decreased uptake and decreased tumor volume.

TABLE 3. Biodistribution of ^{99m}Tc-EC in Breast Tumor-Bearing Rats

	% of injected ^{99m} Tc-EC dose per gram of tissue weight ¹			
	30 min	1 h	2 h	4 h
Blood	0.435±0.029	0.273±0.039	0.211±0.001	0.149±0.008
Lung	0.272±0.019	0.187±0.029	0.144±0.002	0.120±0.012
Liver	0.508±0.062	0.367±0.006	0.286±0.073	0.234±0.016
Stomach	0.136±0.060	0.127±0.106	0.037±0.027	0.043±0.014
Kidney	7.914±0.896	8.991±0.268	9.116±0.053	7.834±1.018
Thyroid	0.219±0.036	0.229±0.118	0.106±0.003	0.083±0.005
Muscle	0.060±0.006	0.043±0.002	0.028±0.009	0.019±0.001
Intestine	0.173±0.029	0.787±0.106	0.401±0.093	0.103±0.009
Urine	9.124±0.808	11.045±6.158	13.192±4.505	8.693±2.981
Tumor	0.342±0.163	0.149±0.020	0.115±0.002	0.096±0.005
Tumor/Blood	0.776±0.322	0.544±0.004	0.546±0.010	0.649±0.005
Tumor/Muscle	5.841±3.253	3.414±0.325	4.425±1.397	5.093±0.223
Tumor/Lung	1.256±0.430	0.797±0.022	0.797±0.002	0.798±0.007

1. Each rat was given 10 µg of ^{99m}Tc-EC. Values shown represent the mean±standard deviation of data from 3 animals.

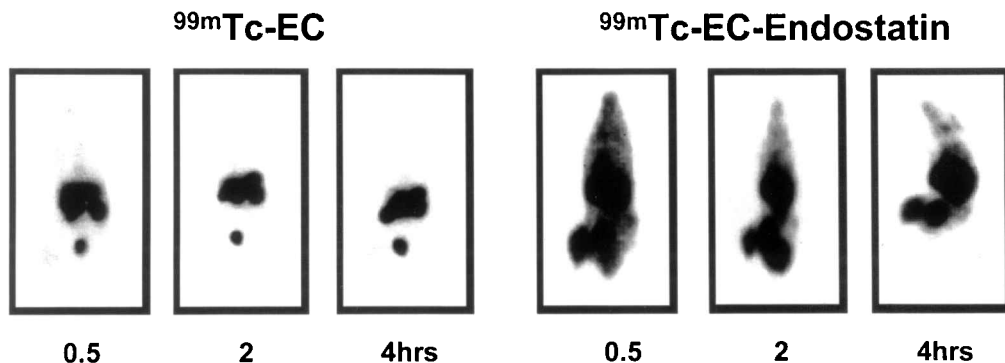


Figure 4. Scintigraphic images of mammary-tumor bearing rats following administration of $^{99m}\text{Tc-EC}$ -endostatin and $^{99m}\text{Tc-EC}$ ($100\ \mu\text{Ci}/10\ \mu\text{g}/\text{rat}$, i.v.) at 0.5–4.0 hrs on day 14 after inoculation of tumor cells. Tumor, located in right hind leg, was well visualized with $^{99m}\text{Tc-EC}$ -endostatin.

In-Situ Hybridization (ISH) Assays

Immunohistochemical staining of tumor cross-section indicated reduced expression (by visualization) of tumor VEGF, bFGF, IL-8 and microvessel density on day 2 post-endostatin treatment as compared to pre-treatment (Figure 8).

DISCUSSION

Studies have suggested neovascularization as a requirement for primary tumor growth, invasion,

and metastasis. Reports also give evidence that acquisition of the angiogenic phenotype is a common pathway for tumor progression, and that active angiogenesis is associated with other molecular mechanisms leading to tumor progression.^{20–23} Antiangiogenic therapy agents, such as endostatin, represent some of the more promising new approaches to anticancer therapy. Endostatin causes apoptosis in endothelial cells, hindering tumor progress. Though measuring angiogenesis (blood vessel density) and/or its

$^{99m}\text{Tc-EC}$ -Nonspecific Peptide

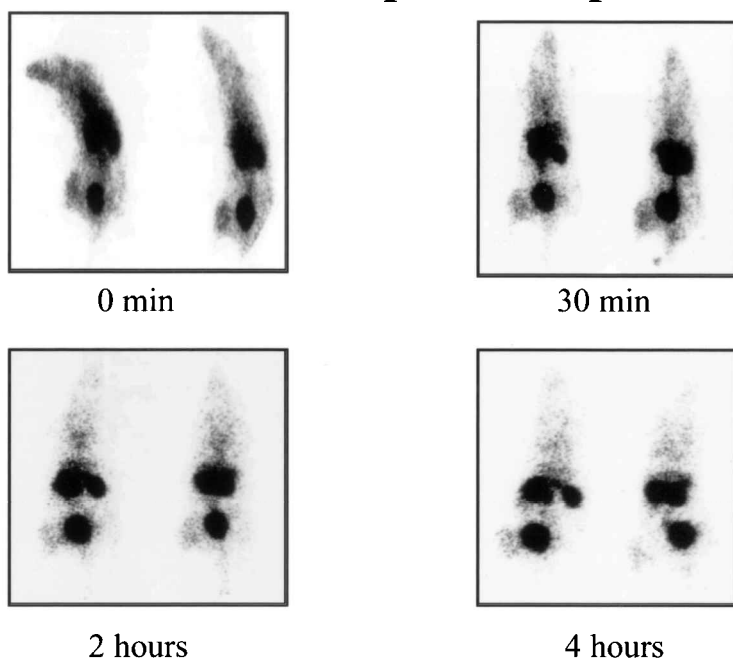


Figure 5. Scintigraphic images of mammary-tumor bearing rats following administration of $^{99m}\text{Tc-EC-K1XaK2tPA}$ ($100\ \mu\text{Ci}/10\ \mu\text{g}/\text{rat}$, i.v.) at 0.5–4.0 hrs on day 14 after inoculation of tumor cells. Tumor, located in right hind leg, was visualized at 0.5 hr, but not at 2–4 hrs.

Anti-tumor Activity of Paclitaxel and Endostatin Against Rat's Mammary Tumor (13762)

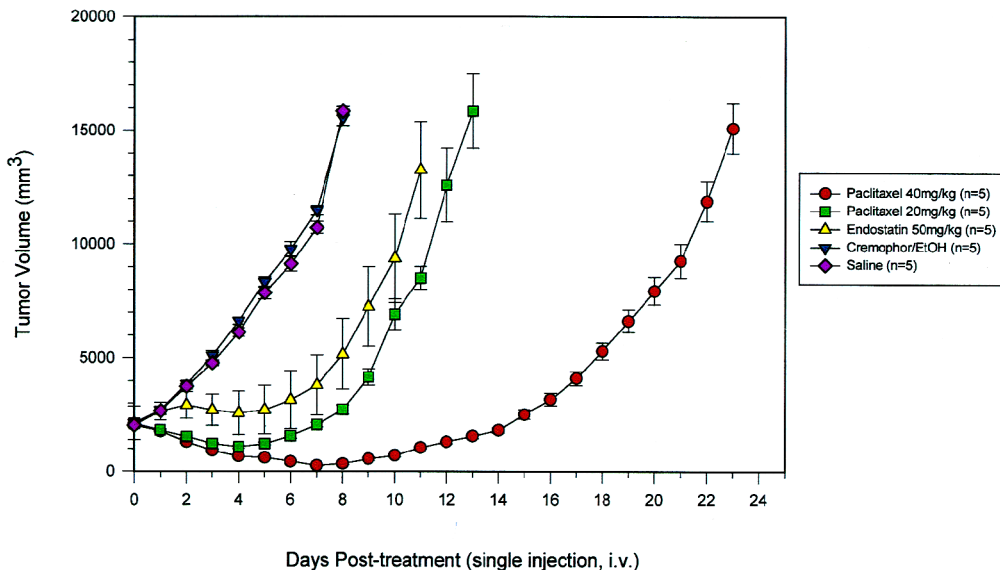


Figure 6. Mammary tumor-bearing rats were dosed a single injection of endostatin (50 mg/kg) or paclitaxel (20 and 40 mg/kg) intravenously. The weights of tumors at sacrifice on day 7 post-treatment were 5.5 ± 0.33 g, 3.1 ± 0.11 g, and 7.9 ± 0.42 g, respectively.

main regulators such as IL-8, VEGF and bFGF in solid tumors may provide new and sensitive markers for tumor progression, metastasis, and prognosis, the therapeutic response of tumors

may not be adequately reflected by these measurements. These invasive methods also have limitations in repeatedly obtaining specimens. ^{99m}Tc -EC-endostatin was synthesized and stud-

Effect of Endostatin and Paclitaxel treatment (day 7) on uptake of ^{99m}Tc -EC-Endostatin in mammary-tumor-bearing rats

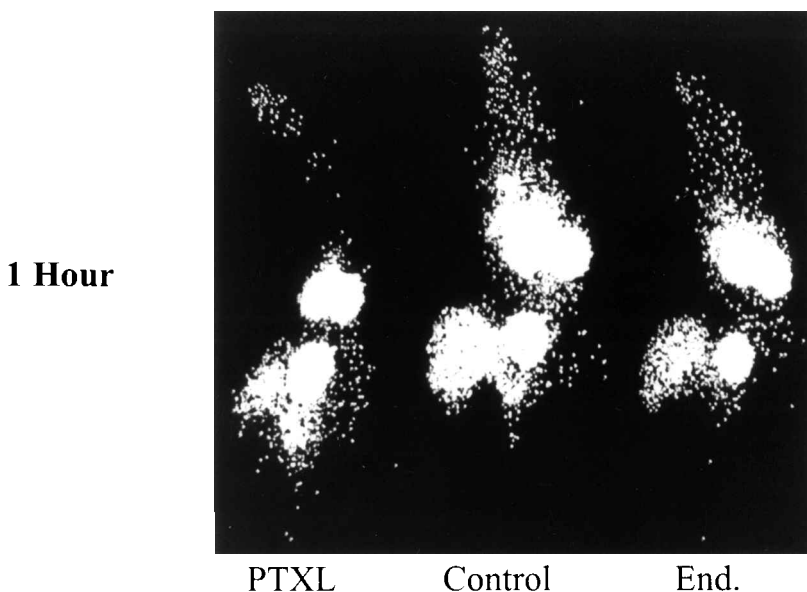


Figure 7. Scintigraphic images of mammary-tumor bearing rats following administration of ^{99m}Tc -EC-endostatin ($10 \mu\text{Ci}/10 \mu\text{g}/\text{rat}$, i.v.) at 1 hr on day 7 after treatment with endostatin (50 mg/kg, i.v.), paclitaxel (20 mg/kg), or saline ($n = 3$ per group).

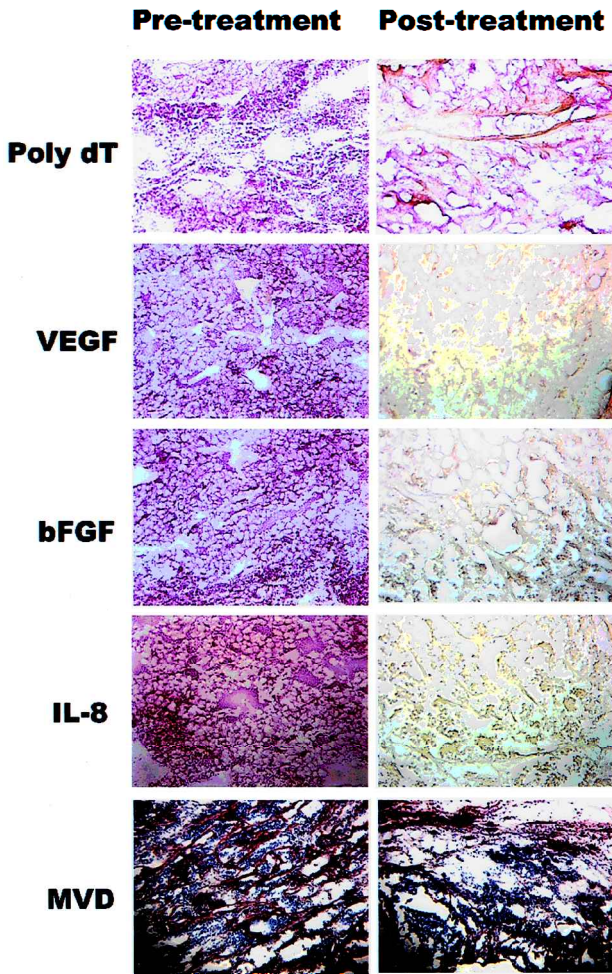


Figure 8. Immunohistochemical staining of tumor sections from mammary tumor-bearing rats treated with a single injection of endostatin (50 mg/kg) intravenously. Tumor specimens were excised at pre- and post-treatment (48 hrs later).

ied for its potential as a noninvasive imaging technique for the evaluation and measurement of tumor response to antiangiogenic therapy.

Despite stability of ^{99m}Tc -EC-endostatin in serum, *in vivo* biodistribution data indicated high kidney uptake and bladder activity. The findings suggest that *in vivo* enzymatic hydrolysis of ^{99m}Tc -EC-endostatin might have occurred. Molecular weight of the fragments of ^{99m}Tc -EC-endostatin is higher than ^{99m}Tc -EC. Higher molecular weight may retain in kidney with a longer time, thus, ^{99m}Tc -EC-endostatin has higher kidney uptake than ^{99m}Tc -EC. Liver uptake in ^{99m}Tc -EC-endostatin groups was higher than ^{99m}Tc -EC groups. The difference in liver uptake may be due to different molecular weight (M.W. 20 kDa of endostatin vs. M.W. 268 of EC). High background in liver and kidneys for ^{99m}Tc -EC-endostatin may limit its clinical application in imaging tumors not in peripheral limbs.

In vitro and *in vivo* cellular uptake studies suggest that endostatin may have its own receptor uptake mechanism. The role of ^{99m}Tc -EC-endostatin in imaging other tumors that overexpress endothelium activity needs to be evaluated. *In vivo* studies revealed that endostatin was less potent than paclitaxel at the doses tested in this model. The findings suggest that the combination use of endostatin with cytotoxic chemotherapeutic agents or radiation therapy may enhance the efficiency of endostatin therapy. However, radiolabeled endostatin was found to be useful as a biological response marker in assessing endostatin therapy. Scintigraphic images showed good visualization of tumor, as well as a correlation between tumor uptake and treatment effects. Decreased tumor-to-nontumor uptake of radiolabeled endostatin following endostatin or paclitaxel treatment correlated to decreased tumor volume as well as decreased expression of an-

giogenic factors. In other words, the decrease in tumor uptake of ^{99m}Tc -EC-endostatin signified effective anti-tumor activity. To ascertain which patients should be under endostatin therapy, a threshold tumor uptake of ^{99m}Tc -EC-endostatin and therapeutic response of endostatin need to be evaluated and that may assist in prediction of efficiency for endostatin therapy.

In summary, a convenient and simple method for radiolabeling endostatin to a high specific activity was achieved. *In vitro* and *in vivo* cellular uptake and planar imaging studies demonstrated the pharmacokinetic distribution and feasibility of using this radiolabeled endostatin to image tumors. Therapeutic response of endostatin and antiangiogenic (e.g., paclitaxel) therapy was assessed by using ^{99m}Tc -EC-endostatin. There was a positive correlation between tumor uptake and angiogenic factor expression. The findings suggest that ^{99m}Tc -EC-endostatin, a specific marker for endothelial cells, may be useful in assessing the outcome of antiangiogenic treatment.

ACKNOWLEDGMENTS

The authors wish to thank Eloise Daigle for her secretarial support. This work was supported in part by the John S. Dunn Foundation and EntreMed Research Fund (SR 00-248). The animal research is supported by M. D. Anderson Cancer Center (CORE) Grant NIH CA-16672.

REFERENCES

- Bertolini F, Paolucci M, Peccatori F, Cinieri S, Agazzi A, Ferrucci PF, Cocorocchio E, Goldhirsch A and Martinelli G. Angiogenic growth factors and endostatin in non-Hodgkin's lymphoma. *Br J Haematol* 1999;106:504-09.
- Cao Y. Therapeutic potentials of angiostatin in the treatment of cancer. *Haematologica* 1999;84:643-50.
- Smith BD, Smith GL, Carter D, Sasaki CT and Haffty BG. Prognostic significance of vascular endothelial growth factor protein levels in oral and oropharyngeal squamous cell carcinoma. *J Clin Oncol* 2000;18:2046-52.
- Jiang L, Jha V, Dhanabal M, Sukhatme VP and Alper SL. Intracellular Ca^{2+} signaling in endothelial cells by the angiogenesis inhibitors endostatin and angiostatin. *Am J Physiol Cell Physiol* 2001;280:1140-50.
- Dhanabal M, Ramchandran R, Waterman MJ, Lu H, Knebelmann B, Segal M and Sukhatme VP. Endostatin induces endothelial cell apoptosis. *J Biol Chem* 1999;274:11721-6.
- Moulton KS, Heller E, Konerding MA, Flynn E, Palinski W and Folkman J. Angiogenesis inhibitors endostatin or TNP-470 reduce intimal neovascularization and plaque growth in apolipoprotein E-deficient mice. *Circulation* 1999;99:1726-32.
- Jouan V, Canon X, Alemany M, Caen JP, Quentin G, Plouet J and Bikfalvi A. Inhibition of *in vitro* angiogenesis by platelet factor-4-derived peptides and mechanism of action. *Blood* 1999;94:984-93.
- Logothetis CJ, Wu KK, Finn LD, Daliani D, Figg W, Ghaddar H and Gutterman JU. Phase I trial of the angiogenesis inhibitor TNP-470 for progressive androgen-independent prostate cancer. *Clin Cancer Res* 2001;7:1198-203.
- Moreira AL, Friedlander DR, Shif B, Kaplan G and Zazgag D. Thalidomide and a thalidomide analogue inhibit endothelial cell proliferation *in vitro*. *J Neurooncol* 1999;43:109-14.
- Duda DG, Sunamura M, Lozonschi L, Kodama T, Egawa S, Matsumoto G, Shimamura H, Shibuya K, Takeda K and Matsuno S. Direct *in vitro* evidence and *in vivo* analysis of the antiangiogenesis effects of interleukin 12. *Cancer Res* 2000;60:1111-6.
- Bocci G, Danesi R, Benelli U, Innocenti F, Di Paolo A, Fogli S and Del Tacca M. Inhibitory effect of suramin in rat models of angiogenesis *in vitro* and *in vivo*. *Cancer Chemother Pharmacol* 1999;43:205-12.
- Sakamoto T, Ishibashi T, Kimura H, Yoshikawa H, Spee C, Harris MS, Hinton DR and Ryan SJ. Effect of tecogalan sodium on angiogenesis *in vitro* by choroidal endothelial cells. *Invest Ophthalmol Vis Sci* 1995;36:1076-83.
- Pedram A, Razandi M and Levin ER. Natriuretic peptides suppress vascular endothelial cell growth factor signaling to angiogenesis. *Endocrinology* 2001;142:1578-86.
- Lozonschi L, Sunamura M, Kobari M, Egawa S, Ding L and Matsuno S. Controlling tumor angiogenesis and metastasis of C26 murine colon adenocarcinoma by a new matrix metalloproteinase inhibitor, KB-R7785, in two tumor models. *Cancer Res* 1999;59:1252-8.
- Maekawa R, Maki H, Yoshida H, Hojo K, Tanaka H, Wada T, Uchida N, Takeda Y, Kasai H, Okamoto H, Tsuzuki H, Kambayashi Y, Watanabe F, Kawada K, Toda K, Ohtani M, Sugita K and Yoshioka T. Correlation of antiangiogenic and antitumor efficacy of N-biphenyl sulfonyl-phenylalanine hydroxamic acid (BPHA), an orally-active, selective matrix metalloproteinase inhibitor. *Cancer Res* 1999;59:1231-5.
- Banerjee SK, Zoubine MN, Sarkar DK, Weston AP, Shah JH and Campbell DR. 2-Methoxyestradiol blocks estrogen-induced rat pituitary tumor growth and tumor angiogenesis: possible role of vascular endothelial growth factor. *Anticancer Res* 2000;20:2641-5.
- Liao F, Li Y, O'Connor W, Zanetta L, Bassi R, Santiago A, Overholser J, Hooper A, Mignatti P, Dejana E, Hicklin DJ and Bohlen P. Monoclonal antibody to vascular endothelial-cadherin is a potent inhibitor of an-

- giogenesis, tumor growth, and metastasis. *Cancer Res* 2000;60:6805-10.
18. Yeh CH, Peng HC, Yang RS and Huang TF. Rhodostomin, a snake venom disintegrin, inhibits angiogenesis elicited by basic fibroblast growth factor and suppresses tumor growth by a selective $\alpha(v)\beta(3)$ blockade of endothelial cells. *Mol Pharmacol* 2001;59:1333-42.
 19. Gasparini G. The rationale and future potential of angiogenesis inhibitors in neoplasia. *Drugs* 1999;58:17-38.
 20. Sion-Vardy N, Fliss DM, Prinsloo I, Shoham-Vardi I and Benharroch D. Neoangiogenesis in squamous cell carcinoma of the larynx—biological and prognostic associations. *Pathol Res Pract* 2001;197:1-5.
 21. Guang-Wu H, Sunagawa M, Jie-En L, Shimada S, Gang Z, Tokeshi Y and Kosugi T. The relationship between microvessel density, the expression of vascular endothelial growth factor (VEGF), and the extension of nasopharyngeal carcinoma. *Laryngoscope* 2000;110:2066-9.
 22. Xiangming C, Hokita S, Natsugoe S, Tanabe G, Baba M, Takao S, Kuroshima K and Aikou T. Angiogenesis as an unfavorable factor related to lymph node metastasis in early gastric cancer. *Ann Surg Oncol* 1998;5:585-9.
 23. Ugurel S, Rappl G, Tilgen W and Reinhold U. Increased serum concentration of angiogenic factors in malignant melanoma patients correlates with tumor progression and survival. *J Clin Oncol* 2001;19:577-83.
 24. Lamszus K, Lengler U, Schmidt NO, Stavrou D, Ergun S and Westphal M. Vascular endothelial growth factor, hepatocyte growth factor/scatter factor, basic fibroblast growth factor, and placenta growth factor in human meningiomas and their relation to angiogenesis and malignancy. *Neurosurgery* 2000;46:938-48.
 25. Petzelbauer P, Watson CA, Pfau SE and Pober JS. IL-8 and angiogenesis: evidence that human endothelial cells lack receptors and do not respond to IL-8 in vitro. *Cytokine* 1995;7:267-72.
 26. Smith K, Fox SB, Whitehouse R, Taylor M, Greenall M, Clarke J and Harris AL. Upregulation of basic fibroblast growth factor in breast carcinoma and its relationship to vascular density, oestrogen receptor, epidermal growth factor receptor and survival. *Ann Oncol* 1999;10:707-13.
 27. Inoue K, Slaton JW, Karashima T, Yoshikawa C, Shuin T, Sweeney P, Millikan R and Dinney CP. The prognostic value of angiogenesis factor expression for predicting recurrence and metastasis of bladder cancer after neoadjuvant chemotherapy and radical cystectomy. *Clin Cancer Res* 2000;6:4866-73.
 28. Burian M, Quint C and Neuchrist C. Angiogenic factors in laryngeal carcinomas: do they have prognostic relevance? *Acta Otolaryngol* 1999;119:289-92.
 29. Slaton JW, Inoue K, Perrotte P, El-Naggar AK, Swanson DA, Fidler IJ and Dinney CP. Expression levels of genes that regulate metastasis and angiogenesis correlate with advanced pathological stage of renal cell carcinoma. *Am J Pathol* 2001;158:735-43.
 30. Ramchandran R, Dhanabal M, Volk R, Waterman MJ, Segal M, Lu H, Knebelmann B, and Sukhatme VP. Antiangiogenic activity of restin, NC10 domain of human collagen XV: comparison to endostatin. *Biochem Biophys Res Commun* 1999;255:735-9.
 31. Szabo S, and Sandor Z. The diagnostic and prognostic value of tumor angiogenesis. *Eur J Surg Suppl* 1998;582:99-103.
 32. O'Reilly MS, Boehm T, Shing TY, Fukai N, Vasios G, Lane WS, Flynn E, Birkhead JR, Olsen BR, and Folkman J. Endostatin: an endogenous inhibitor of angiogenesis and tumor growth. *Cell* 1997;88:277-85.
 33. Gibaldi M. Regulating angiogenesis: a new therapeutic strategy. *J Clin Pharmacol* 1998;38:898-903.
 34. Zetter BR. Angiogenesis and tumor metastasis. *Annu Rev Med* 1998;49:407-24.
 35. De Schepper AM, De Beuckeleer L, Vandevenne J, and Somville J. Magnetic resonance imaging of soft tissue tumors. *Eur Radiol* 2000;10:213-23.
 36. Nowak B, Di Martino E, Janicke S, Cremerius U, Adam G, Zimny M, Reinartz P, and Bull U. Diagnostic evaluation of malignant head and neck cancer by F-18-FDG PET compared to CT/MRI. *Nuklearmedizin* 1999;38:312-18.
 37. Kihlstrom L, and Karlsson B. Imaging changes after radiosurgery for vascular malformations, functional targets, and tumors. *Neurosurg Clin N Am* 1999;10:167-80.
 38. Barker FG, Chang SM, Valk PE, Pounds TR, and Prados MD. 18-Fluorodeoxyglucose uptake and survival of patients with suspected recurrent malignant glioma. *Cancer* 1997;79:115-26.
 39. Yang DJ, Ilgan S, Higuchi T, Zareneyrizi F, Oh CS, Liu CW, Kim EE, and Podoloff DA. Noninvasive assessment of tumor hypoxia with ^{99m}Tc -labeled metronidazole. *Pharm Res* 1999;16:743-50.
 40. Ilgan S, Yang DJ, Higuchi T, Zareneyrizi F, Bayhan H, Yu DF, Kim EE, and Podoloff DA. ^{99m}Tc -Ethylenedicysteine-Folate: A new tumor imaging agent. Synthesis, labeling and evaluation in animals. *Cancer Biotherapy and Radiopharm* 1998;13:427-35.
 41. Zareneyrizi F, Yang DJ, Oh CS, Ilgan S, Yu DF, Tansey W, Liu CW, Kim EE, and Podoloff DA. Synthesis of ^{99m}Tc -ethylenedicysteine-colchicine for evaluation of antiangiogenic effect. *Anti-Cancer Drugs* 1999;10:685-92.
 42. Yang DJ, Azhdarinia A, Wu P, Yu DF, Tansey W, Kohanim S, Kim EE, and Podoloff DA. In vivo and in vitro measurement of apoptosis in breast cancer cells using ^{99m}Tc -EC-annexin V. *Cancer Biotherapy and Radiopharmaceuticals* 2001;16:73-84.
 43. Perletti G, Concari P, Giardini R, Marras E, Piccinini F, Folkman J, and Chen L. Antitumor activity of endostatin against carcinogen-induced rat primary mammary tumors. *Cancer Res* 2000;60:1793-96.
 44. Sim BKL, Fogler WE, Zhou XH, Liang H, Madsen JW,

- Luu K, O'Reilly MS, Tomaszewski JE, Fortier AH. Zinc ligand-disrupted recombinant human endostatin: Potent inhibition of tumor growth, safety and pharmacokinetic profile. *Angiogenesis* 1999;3:41-51.
45. Stodilka RZ, Kemp BJ, Prato FS, Kertesz A, Kuhl D, and Nicholson RL. Scatter and attenuation correction for brain SPECT using attenuation distributions inferred from a head atlas. *J Nucl Med* 2000;41:1569-78.
46. Kao CH, ChangLai SP, Chieng PU, and Yen TC. Technetium-^{99m} methoxyisobutylisocyantrile chest imaging of small cell lung carcinoma: relation to patient prognosis and chemotherapy response—a preliminary report. *Cancer* 1998;83:64-8.
47. Fasciani A, D'Ambrogio G, Bocci G, Monti M, Genazani AR and Artini PG. High concentrations of the vascular endothelial growth factor and interleukin-8 in ovarian endometriomata. *Mol Hum Reprod* 2000; 6:50-4.
48. Pataky DM, Borisoff JF, Fernandes KJ, Tetzlaff W, and Steeves JD. Fibroblast growth factor treatment produces differential effects on survival and neurite outgrowth from identified bulbospinal neurons in vitro. *Exp Neurol* 2000;163:357-72.
49. Radinsky R, Bucana CD, Ellis LM, et al: A rapid colorimetric in situ messenger RNA hybridization technique for analysis of epidermal growth factor receptor in paraffin-embedded surgical specimens of human colon carcinomas. *Cancer Research* 1993;53:937-43.
50. Bucana CD, Fabra A, Sanchez R, et al. Different patterns of macrophage infiltration into allogeneic-murine and xenogeneic-human neoplasms growing in nude mice. *American Journal of Pathology* 1992;141: 1225-36.
51. Pearson WR, Lipman DJ: Improved tools for biological sequence comparison. *Proceedings of the National Academy of Sciences of the United States of America* 1988;85:2444-48.
52. Wild R, Ramakrishnan S, Sedgewick J and Griffioen AW. Quantitative assessment of angiogenesis and tumor vessel architecture by computer-assisted digital image analysis: effects of VEGF-toxin conjugate on tumor microvessel density. *Microvasc Res* 2000;59:368-76.